Front. Energy 2020, 14(3): 443–451
https://doi.org/10.1007/s11708-020-0683-2

RESEARCH ARTICLE

Quan CAO, Dongyan XU, Huanfei XU, Shengjun LUO, Rongbo GUO

Efficient promotion of methane hydrate formation and elimination of foam generation using fluorinated surfactants

Abstract Methane hydrate preparation is an effective method to store and transport methane. In promoters to facilitate methane hydrate formation, homogeneous surfactant solutions, sodium dodecyl sulfate (SDS) in particular, are more favorable than heterogeneous particles, thanks to their faster reaction rate, more storage capacity, and higher stability. Foaming, however, could not be avoided during hydrate dissociation with the presence of SDS. This paper investigated the ability of five fluorinated surfactants: potassium perfluorobutane sulfonate (PBS), potassium perfluorohexyl sulfonate (PHS), potassium perfluorooctane sulfonate (POS), ammonium perfluorooctane sulfonate (AOS), and tetraethylammonium perfluorooctyl sulfonate (TOS) to promote methane hydrate formation. It was found that both PBS and PHS achieve a storage capacity of 150 (*V*/*V*, the volume of methane that can be stored by one volume of water) within 30 min, more than that of SDS. Cationic ions and the carbon chain length were then discussed on their effects during the formation. It was concluded that PBS, PHS, and POS produced no foam during hydrate dissociation, making them promising promoters in large-scale application.

Keywords methane hydrate, fluorinated surfactants, homogeneous promoter, foam elimination, stability

Received Nov. 14, 2019; accepted Apr. 8, 2020; online Jul. 10, 2020

Quan CAO (✉), Shengjun LUO (✉)
Shandong Industrial Engineering Laboratory of Biogas Production and Utilization, Key Laboratory of Biofuels of Chinese Academy of Sciences, Qingdao Institute of Bioenergy and Bioprocess Technology, Chinese Academy of Sciences, Qingdao 266101, China
E-mails: caoquan@qibebt.ac.cn (Quan CAO); luosj@qibebt.ac.cn (Shengjun LUO)

Dongyan XU
Faculty of Engineering, Qingdao University of Science and Technology, Qingdao 266042, China

Huanfei XU
Faculty of Engineering, Qingdao University of Science and Technology, Qingdao 266042, China; College of Chemical Engineering, Qingdao University of Science and Technology, Qingdao 266042, China

Rongbo GUO (✉)
Shandong Industrial Engineering Laboratory of Biogas Production and Utilization, Key Laboratory of Biofuels of Chinese Academy of Sciences, Qingdao Institute of Bioenergy and Bioprocess Technology, Chinese Academy of Sciences, Qingdao 266101, China; Dalian National Laboratory for Clean Energy, Dalian 116023, China; Faculty of Engineering, Qingdao University of Science and Technology, Qingdao 266042, China
E-mails: guorb@qibebt.ac.cn

1 Introduction

Methane, as a clean energy source, has been applied not only in people's daily life, but also plays a crucial part in the traffic and chemical industry. It is estimated that its natural reserve can serve mankind for as long as 1000 years [1,2]. Producing methane by fermentation with waste and straw was a great breakthrough [3–7]. However, methane storage and transportation are two major challenges due to the fact that methane molecules can only be liquefied at a very low temperature of –161.5°C at atmospheric pressure [8]. Methane hydrate is an ice-like compound composed of methane molecule in the cage crystal center surrounded by water molecules with non-stoichiometric mole ratio [9–11]. It has been, therefore, considered as a potential compound to store methane under mild conditions. One volume of water could theoretically store 172 volumes of methane in maximum for methane hydrate [12]. Methane hydrate can be stored at –20°C for 3 months at atmospheric pressure [13,14]. As increasing attention has been paid to methane hydrate synthesis, great progress has been made. Promoters are necessary to facilitate methane hydrate formation. These surfactants able to reduce the surface tension of water in an aqueous solution have been proved to be excellent promoters [15–20]. Among the surfactants, anionic ones, especially those bearing sulfate or sulfonate groups, including sodium dodecyl sulfate (SDS) and sodium dodecyl sulfonate (AS) are excellent choices due to their fast reaction rate and high storage capacity [21–23].

However, both of the two surfactants would generate large quantities of foam during hydrate dissociation [24,25]. Foaming would lead to loss of surfactants and pollution on the equipment, which further affect their recycling. Lower surfactant concentration is a method to eliminate the foam. But this will significantly reduce its activity. In addition, heterogeneous promoters have also been developed. For instance, amphiphilic-polymer-coated carbon nanotubes, grafting of nano-Ag particles on $-SO_3^-$ coated nanopolymers, $-SO_3^-$ coated graphene oxide nanosheets and $-SO_3^-$ coated nanopromoters have been employed as methane hydrate promoters which largely alleviated foam formation [26–32]. Nevertheless, the above heterogeneous promoters are inferior to SDS in methane hydrate formation rate. Besides, long-term storage stability is another challenge for their utilization. It is hence necessary to develop novel homogeneous promoters with both a fast reaction rate and a low foam generation. Wang et al. have compared the activity of SDS with sodium dodecyl benzene sulfonate (SDBS) in methane hydrate formation. They have found that the surface tension and contact angle are two factors affecting the formation rate and growth pattern of the hydrate [33]. SDS with a weaker surface tension and a smaller contact angle shows a faster hydrate growth than SDBS. The difference between SDS and SDBS in wettability makes their hydrate growth one upward and the other only at the bottom of the reactor [33]. Foam eventually breaks down due to its instability. For a surfactant with a long alkyl chain length as SDS, its foam would be around for a long time owing to the weak surface tension and high film strength. To alleviate foam generation, surfactants with a shorter alkyl chain length are better choices than those longer ones. But they are inefficient in reducing the surface tension and contact angle [34], resulting in low activities in methane hydrate formation.

Fluorinated surfactants (FS) are known to be more surface active than hydrocarbon surfactants (HS) even if their carbon chain length is shorter than that of HS [35,36]. However, their application in methane hydrate has not been studied yet. In this paper, commercial FS bearing the sulfonic group are employed as promoters for methane hydrate formation. The effects of their carbon chain length and cationic ions on reaction rate, methane storage capacity and foam generation are also discussed.

2 Experimental section

2.1 Materials

The potassium perfluorobutane sulfonate (PBS), potassium perfluorohexyl sulfonate (PHS), potassium perfluorooctane sulfonate (POS), ammonium perfluorooctane sulfonate (AOS), and tetraethylammonium perfluorooctyl sulfonate (TOS) used in the experiment were produced by Wuhan Silworld Chemical Co., Ltd., China. The sodium dodecyl sulfate (SDS), KCl, NH_4Cl and KOH were produced by China National Pharmaceutical Group Co., Ltd., China. The tetraethyl ammonium hydroxide (25% aqueous solution) was produced by Yancheng FineChem Co., Ltd., China. The deionized water with a conductivity of less than 0.014 μs/cm at 293.15 K was made in the laboratory where the experiment was conducted.

2.2 Characterization methods

The surface tension of the fluorinated surfactant solution was measured using a Teclis Tracker HT-HP surface tension tester. The contact angle of the surfactant solution with the vessel wall was measured using a JC2000D1 contact angle analyzer. The viscosities of the surfactant solutions were analyzed using a Brookfield DV2T viscometer at 100 r/min.

2.3 Methane hydrate formation

The methane hydrate was prepared in an 80 mL autoclave made of 316 L stainless steel with a maximum pressure capability of 20 MPa. In a typical reaction, 10 mL of surfactant solution was charged into the autoclave which was sealed and placed in a thermostatic water bath. After reaching the desired temperature, the reactor was purged three times with methane and pressurized to a certain pressure. Then, stirring started at 300 r/min. The evolution of the pressure and temperature during methane hydrate formation was recorded by a computer. The schematic representation of the methane hydrate formation apparatus was shown in Scheme 1.

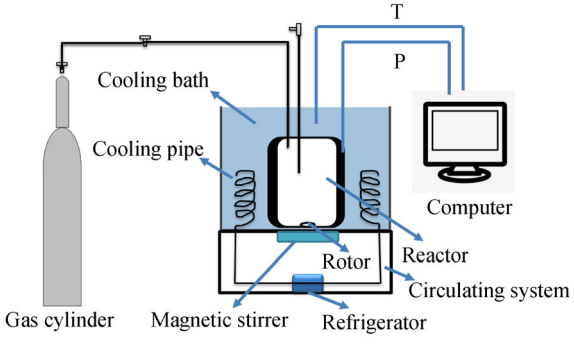

Scheme 1 Graphical representation of hydrate formation apparatus.

After the methane pressure reached a constant value, the unreacted methane gas in the vessel was released at atmospheric pressure. Then the vessel was taken out from the cooling bath and opened immediately to observe the morphology of the methane hydrate formed. The whole process was completed within two minutes.

The methane consumed at time t (n_t) in the methane

hydrate formation process was defined as the mole of methane required per mL of water. n_t was calculated according to the following formulas which were derived by Wang et al. [32,37].

$$n_t = \frac{\frac{P_0V_0}{Z_0RT_0} - \frac{P_tV_0}{Z_tRT_t}}{V_W\left(1 - \frac{P_t\Delta V_m}{Z_tRT_t}\right)}, \quad (1)$$

$$Z_t = 1 + \left[0.083 - 0.422 \times \left(\frac{T_c}{T_t}\right)^{1.6}\right]\frac{P_tT_c}{P_cT_t} + \omega\left[0.139 - 0.172 \times \left(\frac{T_c}{T_t}\right)^{4.2}\right]\frac{P_tT_c}{P_cT_t}, \quad (2)$$

where P_0, V_0, and T_0 represent the pressure, the volume, and the temperature of the gas phase at time 0; P_t, V_t, and T_t represent the pressure, the volume, and the temperature at time t; R, m, and ΔV represent the universal gas constant, the hydration number, and the molar volume difference between water and methane hydrates, which has been reported to be 4.6 cm^3 per mole of water; and Z_0 and Z_t represent the compressibility factor at time 0 and t. P_c and T_c represent critical pressure and critical temperature respectively. For methane, ω, P_c, and T_c are 0.012, 4.599 MPa, and 190.6 K, respectively according to the literature.

The methane storage capacity (C_s) corresponding to the volume of methane that can be stored by one volume of water (V/V) of the methane hydrates formed at time t can be calculated by using

$$C_s = \frac{n_t \times V_{mg} \times V_{mw}}{V_w \times (V_{mw} + \Delta V)}, \quad (3)$$

where n_t, V_{mg} and V_{mw} represent the methane consumption at time t, the molar volume of gas and the molar volume of water at standard temperature and pressure; V_w is the volume of water used in gas hydrate formation; and ΔV is the molar volume difference between hydrates and water.

3 Results and discussion

3.1 Measurement of surface tension and contact angle

According to the conclusions drawn by Wang et al., the SDS with a weaker surface tension and a smaller contact angle than that of SDBS results in a faster reaction rate, a higher methane storage capacity, and an upward hydrate growth pattern, because of the fact that a weak surface tension is beneficial for the diffusion of methane from the gas to the liquid phase and is thus favorable for the contact of methane with water [33]. Correspondingly, a weaker surface tension results in a smaller contact angle and water is sucked up along the side wall of the reactor due to the capillary effect. That is the reason for the growth of the hydrate obtained from SDBS with a low contact angle only at the bottom of the reactor. Therefore, the surface tension and contact angle of the surfactant solution of fluorinated surfactants were investigated owing to their important role in hydrate formation with the results shown in Figs. 1 and 2.

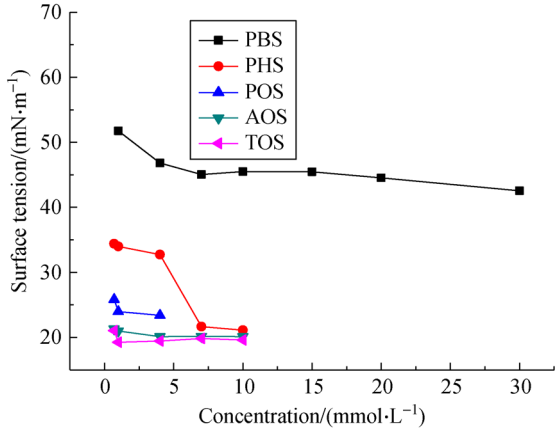

Fig. 1 Surface tension of fluorinated surfactants at 20°C.

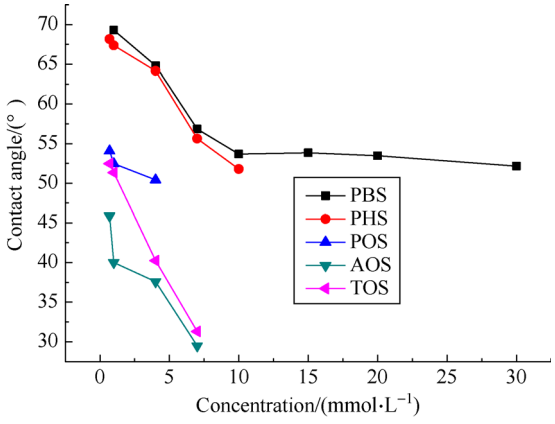

Fig. 2 Contact angles of fluorinated surfactant solutions at 20°C.

In Fig. 1, the surface tension decreases upon increasing the surfactant concentration before it reaches a nearly constant value, revealing that the micelles are formed [38]. At the same concentration, for example 4 mmol/L, the surface tension decreases following the order of PBS, PHS, POS, AOS, and TOS. This is predictable because a longer C–F chain would make the surfactant more easily adsorbed at the interface, which reduces the surface tension [38]. The minimum surface tension for PBS, PHS, POS, AOS, and TOS are around 42, 21, 23, 20, and 19 mN/m respectively. The counter-ions could compress the double-layer of the surfactants and make them combine closely [39]. Therefore, the surface tension and critical micelle

concentration are reduced after the addition of salts. Figure 1 further demonstrates that NH_4^+ and tetraethylammonium ion are more capable of compressing the double-layer than K^+. Thus the surface tension of AOS and TOS are lower than that of POS at the same concentration.

A weaker surface tension generally leads to a smaller contact angle [39]. Therefore, in Fig. 2, as the concentration increases, the contact angle of all surfactants decreases correspondingly. At the same concentration, the contact angle reduces following the order of PBS, PHS, POS, TOS, and AOS.

3.2 Methane hydrate formation with fluorinated surfactants

The five fluorinated surfactants were all tested for their ability to promote methane hydrate formation as depicted in Fig. 3. In general, the hydrate formation is a two-stage process. The first is called an induction period in which the methane pressure keeps almost at a constant value and the hydrate grows slowly until the nucleus is large enough to initiate the second stage, which is called the growth period [32]. During that time period, the methane pressure decreases quickly. As can be observed in Fig. 3, most of

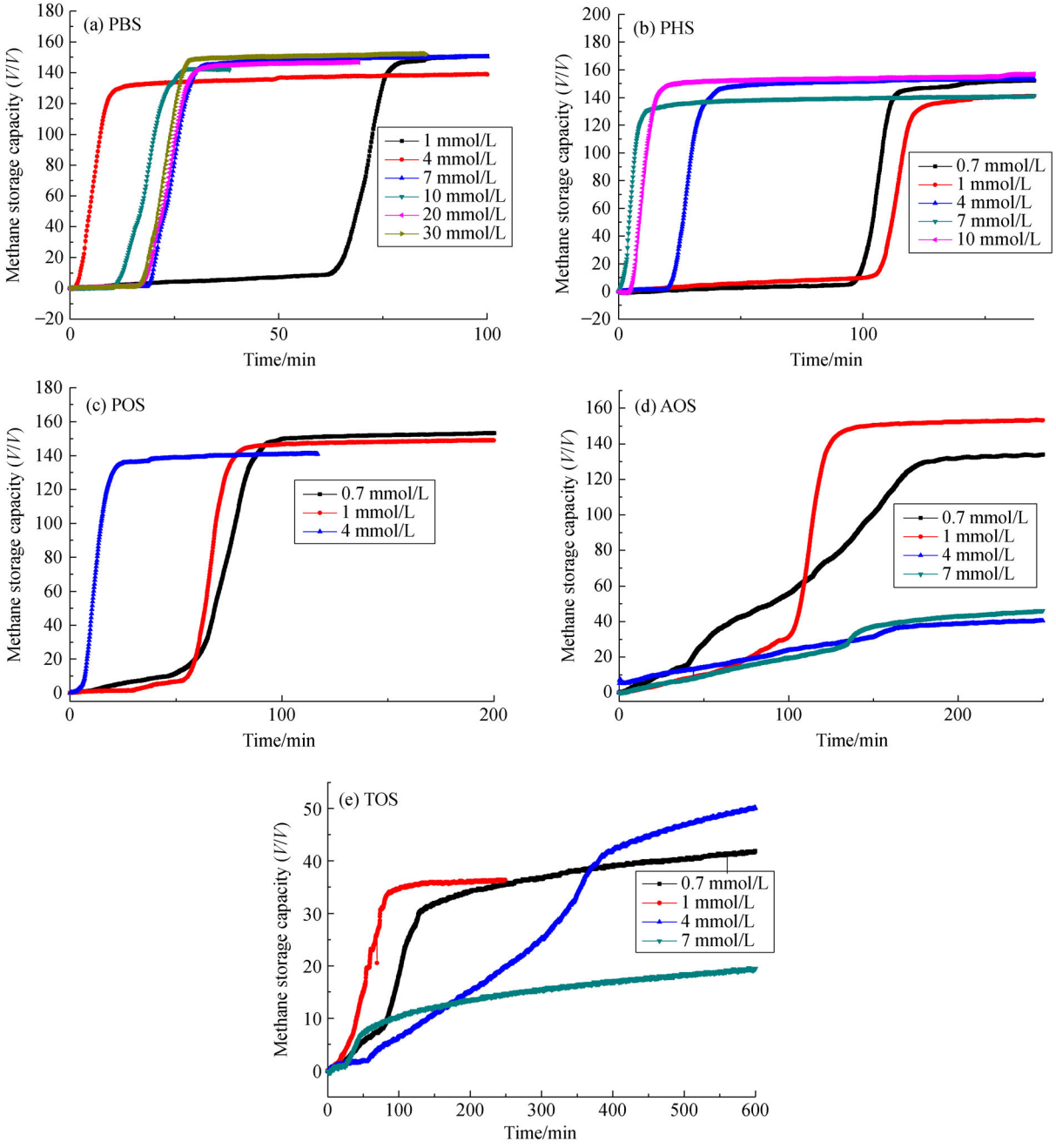

Fig. 3 Methane consumption versus time for fluorinated surfactants at 300 r/min, a temperature of 2°C, and a pressure of 6 MPa.

the FS changes slightly in methane storage for some time and then increases sharply until reaching a plateau. The induction time and maximum methane storage capacity are listed in Table S1 (Electronic Supplementary Material).

For PBS, at a low concentration of 1 mmol/L, the induction time needed is as long as 65 min. But increasing the concentration from 1 mM to 30 mM would shorten the induction time. Since the surfactant could facilitate the formation of methane hydrate, increasing its concentration would theoretically lead to a shorter induction time and a higher methane storage capacity. However, as revealed in Fig. 3 and Table S1, a higher concentration of the surfactant would not necessarily lead to a better methane hydrate formation. PBS reaches its minimum induction time at 4 mmol/L while the maximum methane storage capacity is obtained at 30 mmol/L. For PHS, when the concentration is more than 4 mmol/L, a less than 10 min of induction time is needed and the maximum methane storage capacity reaches 156 (*V/V*) at 10 mmol/L. As the solubility of PHS at room temperature could not exceed 13 mmol/L, further increase in its concentration was not investigated. For POS, a minimum induction time of 7 min and a maximum methane storage capacity of 153 (*V/V*) are reached at 4 mmol/L and 0.7 mmol/L respectively. POS is not soluble above 4 mmol/L. Different from the aforementioned three surfactants, AOS achieves a high storage capacity of 152 (*V/V*) at 1 mmol/L. Increasing its concentration to 7 mmol/L results in dramatical decrease in methane storage capacity to only 46 (*V/V*). It is also inferior to PBS, PHS, and POS in promoting rate. In the case of TOS, in the range of 0.7 mmol/L to 7 mmol/L, less than 50 (*V/V*) is achieved even the time is prolonged to 600 min. Under the same reaction condition as that in Fig. S1, it is found that SDS (5 mmol/L and 7 mmol/L) achieves a maximum storage capacity of 141 (*V/V*) in this paper. The above results suggest that PBS, PHS, and POS are more efficient than SDS in methane storage capacity under optimum conditions without considering the concentrations of surfactants.

A weak surface tension makes it easier for methane to diffuse from gas phase to liquid phase, leading to a better contact between methane and water. However, the surface tension alone cannot explain the slow growth rate of AOS and TOS, because both of them are very low in surface tension. Seen from Fig. 3, only AOS at 1 mmol/L achieves a methane storage capacity as high as 152 (*V/V*) within a time as long as 150 min. Increasing the concentration of AOS and TOS from 1 mmol/L to 7 mmol/L does not improve their activities, which could be ascribed to the cations ammonium and tetraethylammonium. To clarify whether the two cations could make the surfactant inert in hydrate formation, ammonium chloride and tetraethylammonium hydroxide (TEAOH) were added into the PHS solution (7 mM) with the results illustrated in Fig. 4. The effects of KCl and KOH were also investigated to rule out the impact of anions Cl^- and OH^- added. From Fig. 4, it is

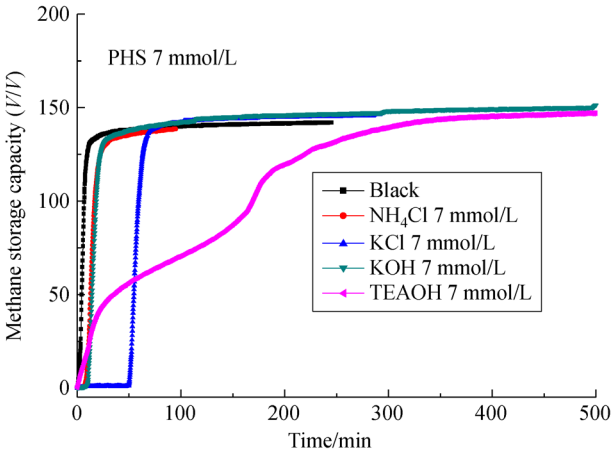

Fig. 4 Effects of salts added on hydration formation at 300 r/min, a temperature of 2°C, and a pressure of 6 MPa.

noticed that the addition of NH_4Cl and KOH does not affect the activity of PHS. KCl only prolongs the induction time but with no impact on the maximum storage capacity. Similar to the results in Fig. 3 (TOS), the addition of TEAOH into PHS solution decreases the hydrate growth. Thus it is concluded that tetraethylammonium ion could make active anion perfluorooctyl sulfonate inert. Different from Fig. 3 (TOS), PHS (7 mmol/L) and TEAOH (7 mmol/L) could still achieve a maximum storage capacity of 144 (*V/V*) after 350 min.

It is not true that a higher concentration of the five fluorinated surfactants would certainly lead to a higher storage capacity. It is the optimum concentration that really achieves the maximum methane storage capacity. The reason for this is that the surfactant itself is a salt which can bound water molecules around it. Therefore, increasing the surfactant concentration blindly will hinder the formation of methane hydrate in this respect.

Except promoters themselves, mass transfer is also an important factor for hydrate formation. Therefore, the viscosities of the surfactant solutions were measured with the results shown in Table 1. PBS (40 mmol/L), PHS (10 mmol/L), POS (4 mmol/L), AOS (1 mmol/L), and

Table 1 Viscosities of surfactant solutions at 20°C

Surfactant	Concentration/(m·mol·L^{-1})	Viscosity/(mPa·S)
PBS	40	2.9
PHS	10	3.1
POS	4	2.8
AOS	1	3.4
AOS	4	6.7
AOS	7	8.2
TOS	1	3.6
TOS	4	7.1
TOS	7	8.7

TOS (1 mmol/L) all have a low viscosity of about 3 mPa·S. Increasing the concentration of AOS and TOS from 1 mmol/L to 7 mmol/L leads to an increase in viscosity from 3 mPa·S to 8 mPa·S. This is due to the growth of micelles from globe to rod and even wormlike [40]. The changes in viscosity may be one reason for the deactivation of AOS and TOS when their concentration increases.

3.3 Foam generation during hydrate dissociation

For aqueous surfactant solutions, when being sloshed or with gas passing through them, foaming becomes an important parameter to evaluate a surfactant used in hydrate production. However, foam is thermodynamically unstable and finally disappears. It was suggested that foam with a lower surface tension, a higher membrane strength and viscosity would last longer [41]. Foam is produced during the process of methane hydrate dissociation. If the foam maintains stable, the continuous gas flow would raise the height of the foam, which explains the fact that when SDS is used as a promoter, the foam would go along the pipe with the gas flow during the dissociation of hydrate. Besides, it is full of foam when the vessel is opened. In the present paper, when PBS, PHSs and POS were employed as promoters, no foam was observed after the reactor was opened as displayed in Fig. 5. The hydrates decomposed in a very smooth way until they completely became homogeneous solutions. But for AOS and TOS, a lot of foam could be seen both in the reactor and gas outlet. All the five FS demonstrated an upward growth pattern. Figure 2 displays their respective contact angles which are all lower than 90°, suggesting the wettability of the solution with the vessel sidewall. Figure 5 demonstrates the foam generated by SDS, AOS, and TOS.

It was observed in Fig. 5 that no foam was generated when the hydrate from PBS, PHS, and POS was dissociated. To better understand the above conclusion, the PBS, PHS, and SDS solutions in transparent glass bottles were violently shaken for ten seconds and then left still for 5 min with their photographs shown in Fig. 6. Figure 6 reveals that the foam produced by PBS at 30 mmol/L has completely vanished. Only a little foam still remain around for PHS at 10 mmol/L. SDS produced a higher foam height than that of PHS at 10 mmol/L even at a low concentration of 1 mmol/L. At 4 mmol/L, the bottle is full of foam. The stability of the foam in Fig. 6 facilitate the further understanding of the reason why PBS, PHS, and POS produces no foam in Fig. 5. It could be explained by the weak film strength of PBS, PHSs and POS resulted from their short carbon chain length. For AOS and TOS, the cations ammonium ion and tetraethylammonium ion could help stabilize the foam.

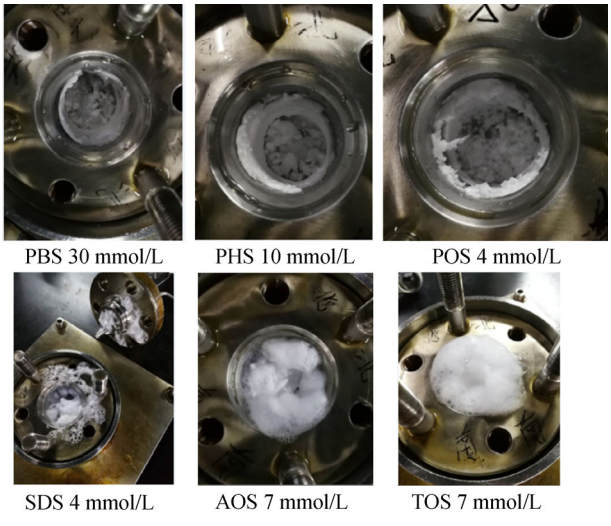

Fig. 5 Photographs of hydrate dissociation.

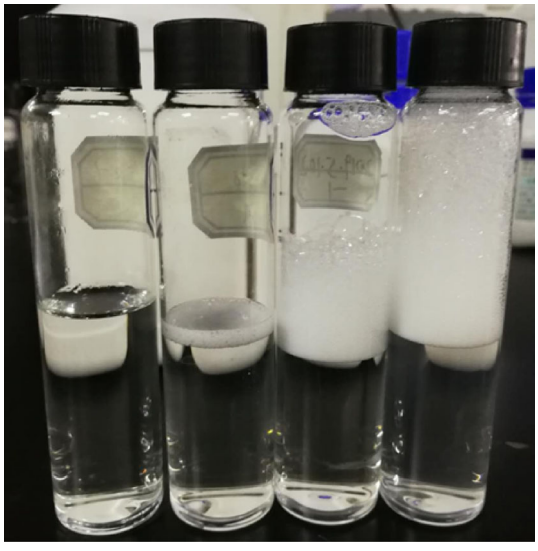

Fig. 6 Photographs taken five minutes after violently shaking the surfactant solutions (from left to right: PBS 30 mmol/L; PHS 10 mmol/L; SDS 1 mmol/L; SDS 4 mmol/L).

3.4 Effects of temperature and pressure

As noticed in Fig. 3, PHS at 10 mmol/L is superior to the other surfactants considering both the reaction rate and storage capacity. It is therefore significant to investigate the effects of temperature and pressure. The results are exhibited in Fig. 7. Increasing the temperature from 2°C to 4°C at an initial pressure of 6 MPa prolongs the induction time from 6 to 215 min and lowers the maximum storage capacity from 156 (*V/V*) to 130 (*V/V*). At the same temperature of 2°C, reducing the initial pressure from 6 to 4 MPa leads to a maximum storage capacity decreasing from 156 (*V/V*) to only 51 (*V/V*). However, when the initial pressure is 3 MPa, no hydrate is formed as indicated by the

drop of the pressure even after 24 h. At a fixed temperature, a minimum pressure is needed to initiate the reaction. The results further verifies the statement that the low temperature and high pressure are favorable for the formation of hydrate. The reason for this is that the high pressure increases the solubility of methane in aqueous solution, and as is known to all, low temperature contributes to the transformation of liquid to solid.

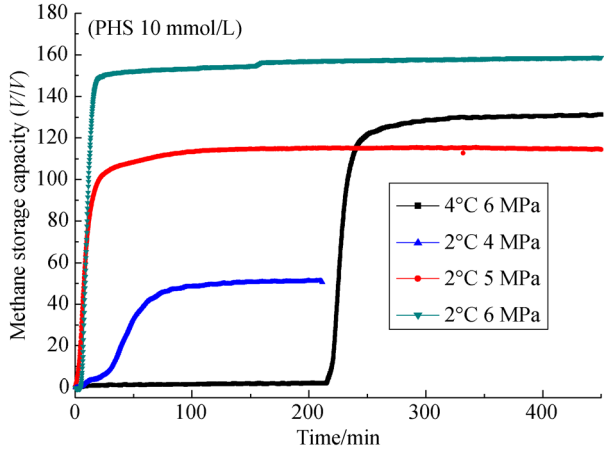

Fig. 7 Hydrate formation at 300 r/min, different temperatures, and pressures.

3.5 Reactions under static conditions and recycling of PHS

Stirring, which facilitated the contact of methane and water and the subsequent hydrate formation, was conducted in all the above experiments. However, if the hydrate formation could be realized under static conditions, it would reduce the cost of the reactor and simplify the process. Therefore, reactions were tried to be performed without stirring. Figure 8 displays the results at PHS 10 mmol/L and its recycling. After releasing the residual methane gas, the vessel was placed at room temperature for two hours to make sure that the dissociation of the hydrate is complete. Then, the next cycle was started. Observed from Fig. 8, a storage capacity of approximately 140 (*V/V*) could be achieved in less than 40 min for PHS (10 mmol/L) even without stirring, only a little inferior to the maximum storage capacity (156 *V/V*) in Fig. 3 under stirring. After being recycled for 5 times, PHS does not lose its activity at all, suggesting its high stability.

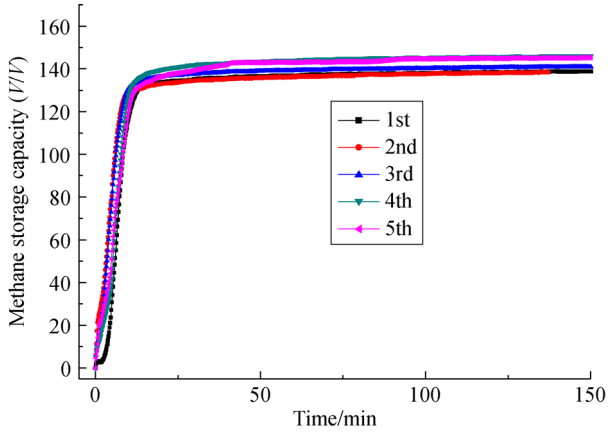

Fig. 8 Reactions with PHS (10 mmol/L) without stirring and its recycling at a temperature of 2°C and a pressure of 6 MPa.

4 Conclusions

Five anionic fluorinated surfactants with sulfonate group were employed as promoters for methane hydration formation. A storage capacity of more than 150 (*V/V*) could be achieved by PBS, PHS, POS, and AOS under optimum conditions. Considering both the reaction rate and storage capacity, PHS (10 mmol/L) demonstrated the best activity. The higher viscosity of AOS and TOS may be one reason for their inactivation. During the dissociation of methane hydrate, foam was eliminated for PBS, PHS, and POS due to the low film strength stabilized by these short carbon-chain surfactants. PHS (10 mmol/L) could achieve a storage capacity of 140 (*V/V*) under static conditions with an excellent stability. The fast reaction rate, high storage capacity, and foam elimination endow PBS, PHS, and POS with great potential in large-scale application in the future.

Acknowledgements This work was financially supported by the Key R&D Project of Shandong Province (No. 2017GSF16106), DICP & QIBEBT Unite Fund (No.: DICP & QIBEBT UN201807) and Strategic Priority Research Program of the Chinese Academy of Science (No. XDA 21060400).

Electronic Supplementary Material Supplementary material is available in the online version of this article at https://doi.org/ 10.1007/s11708-020-0683-2 and is accessible for authorized users.

References

1. Yang M J, Zheng J N, Gao Y, Ma Z, Lv X, Song Y. Dissociation characteristics of methane hydrates in South China Sea sediments by depressurization. Applied Energy, 2019, 243: 266–273
2. Zhang J, Yip C, Xia C, Liang Y. Evaluation of methane release from coals from the San Juan basin and Powder River basin. Fuel, 2019, 244: 388–394
3. Rathi R, Lavania M, Singh N, Sarma P M, Kishore P, Hajra P, Lal B. Evaluating indigenous diversity and its potential for microbial methane generation from thermogenic coal bed methane reservoir. Fuel, 2019, 250: 362–372
4. Wang A, Austin D, Song H. Investigations of thermochemical upgrading of biomass and its model compounds: opportunities for methane utilization. Fuel, 2019, 246: 443–453
5. Guo H, Cheng Y, Huang Z, Urynowicz M A, Liang W, Han Z, Liu J. Factors affecting co-degradation of coal and straw to enhance

biogenic coalbed methane. Fuel, 2019, 244: 240–246
6. Lay C, Vo T, Lin P Y, Abdul P M, Liu C M, Lin C Y. Anaerobic hydrogen and methane production from low-strength beverage wastewater. International Journal of Hydrogen Energy, 2019, 44 (28): 14351–14361
7. Andres-Garcia E, Dikhtiarenko A, Fauth F, Silvestre-Albero J, Ramos-Fernández E V, Gascon J, Corma A, Kapteijn F. Methane hydrates: nucleation in microporous materials. Chemical Engineering Journal, 2019, 360: 569–576
8. Gbaruko B C, Igwe J C, Gbaruko P N, Nwokeoma R C. Gas hydrates and clathrates: flow assurance, environmental and economic perspectives and the Nigerian liquified natural gas project. Journal of Petroleum Science Engineering, 2007, 56(1–3): 192–198
9. Ohmura R, Takeya S, Uchida T, Ebinuma T. Clathrate hydrate formed with methane and 2-propanol: confirmation of structure II hydrate formation. Industrial & Engineering Chemistry Research, 2004, 43(16): 4964–4966
10. Jin Y, Kida M, Konno Y, Nagao J. Clathrate hydrate equilibrium in methane-water systems with the addition of monosaccharide and sugar alcohol. Journal of Chemical & Engineering Data, 2017, 62 (1): 440–444
11. Imasato K, Tokutomi H, Ohmura R. Crystal growth behavior of methane hydrate in the presence of liquid hydrocarbon. Crystal Growth & Design, 2015, 15(1): 428–433
12. Susilo R, Alavi S, Ripmeester J, Englezos P. Tuning methane content in gas hydrates via thermodynamic modeling and molecular dynamics simulation. Fluid Phase Equilibria, 2008, 263(1): 6–17
13. Mimachi H, Takahashi M, Takeya S, Gotoh Y, Yoneyama A, Hyodo K, Takeda T, Murayama T. Effect of long-term storage and thermal history on the gas content of natural gas hydrate pellets under ambient pressure. Energy & Fuels, 2015, 29(8): 4827–4834
14. Takeya S, Yoneyama A, Ueda K, Hyodo K, Takeda T, Mimachi H, Takahashi M, Iwasaki T, Sano K, Yamawaki H, Gotoh Y. Nondestructive imaging of anomalously preserved methane clathrate hydrate by phase contrast X-ray imaging. Journal of Physical Chemistry C, 2011, 115(32): 16193–16199
15. Gupta P, Sakthivel S, Sangwai J S. Effect of aromatic/aliphatic based ionic liquids on the phase behavior of methane hydrates: experiments and modeling. Journal of Chemical Thermodynamics, 2018, 117: 9–20
16. Jadav S, Sakthipriya N, Doble M, Sangwai J S. Effect of biosurfactants produced by Bacillus subtilis and Pseudomonas aeruginosa on the formation kinetics of methane hydrates. Journal of Natural Gas Science and Engineering, 2017, 43: 156–166
17. Ganji H, Manteghian M, Sadaghiani Zadeh K, Omidkhah M R, Rahimi Mofrad H. Effect of different surfactants on methane hydrate formation rate, stability and storage capacity. Fuel, 2007, 86(3): 434–441
18. Erfani A, Fallahjokandan E, Varaminian F. Effects of non-ionic surfactants on formation kinetics of structure H hydrate regarding transportation and storage of natural gas. Journal of Natural Gas Science and Engineering, 2017, 37: 397–408
19. Verrett J, Servio P. Evaluating surfactants and their effect on methane mole fraction during hydrate growth. Industrial & Engineering Chemistry Research, 2012, 51(40): 13144–13149
20. Aliabadi M, Rasoolzadeh A, Esmaeilzadeh F, Alamdari A M. Experimental study of using CuO nanoparticles as a methane hydrate promoter. Journal of Natural Gas Science and Engineering, 2015, 27: 1518–1522
21. Choudhary N, Hande V R, Roy S, Chakrabarty S, Kumar R. Effect of sodium dodecyl sulfate surfactant on methane hydrate formation: a molecular dynamics study. Journal of Physical Chemistry B, 2018, 122(25): 6536–6542
22. Siangsai A, Inkong K, Kulprathipanja S, Kitiyanan B, Rangsunvigit P. Roles of sodium dodecyl sulfate on tetrahydrofuran-assisted methane hydrate formation. Journal of Oleo Science, 2018, 67(6): 707–717
23. Watanabe K, Niwa S, Mori Y H. Surface tensions of aqueous solutions of sodium alkyl sulfates in contact with methane under hydrate-forming conditions. Journal of Chemical & Engineering Data, 2005, 50(5): 1672–1676
24. Bhattacharjee G, Barmecha V, Kushwaha O S, Kumar R. Kinetic promotion of methane hydrate formation by combining anionic and silicone surfactants: scalability promise of methane storage due to prevention of foam formation. Journal of Chemical Thermodynamics, 2018, 117: 248–255
25. Pandey G, Bhattacharjee G, Veluswamy H P, Kumar R, Sangwai J S, Linga P. Alleviation of foam formation in a surfactant driven gas hydrate system: insights via a detailed morphological study. ACS Applied Energy Materials, 2018, 1: 6899–6911
26. Song Y, Wang F, Guo G, Luo S J, Guo R B. Amphiphilic-polymer-coated carbon nanotubes as promoters for methane hydrate formation. ACS Sustainable Chemistry & Engineering, 2017, 5 (10): 9271–9278
27. Wang F, Guo G, Luo S J, Guo R B. Grafting of nano-Ag particles on $-SO_3^-$ -coated nanopolymers for promoting methane hydrate formation. Journal of Materials Chemistry, 2017, 5(35): 18486–18493
28. Wang F, Liu G, Meng H L, Guo G, Luo S J, Guo R B. Improved methane hydrate formation and dissociation with nanosphere-based fixed surfactants as promoters. ACS Sustainable Chemistry & Engineering, 2016, 4(4): 2107–2113
29. Wang F, Meng H, Guo G, Luo S J, Guo R B. Methane hydrate formation promoted by $-SO_3^-$ -coated graphene oxide nanosheets. ACS Sustainable Chemistry & Engineering, 2017, 5(8): 6597–6604
30. Wang F, Guo G, Luo S J, Guo R B. Preparation of $-SO_3^-$ -coated nanopromoters for methane hydrate formation: effects of the existence pattern of $-SO_3^-$ groups on the promotion efficiency. Journal of Materials Chemistry, 2017, 5(6): 2640–2648
31. Song Y, Wang F, Liu G, Luo S, Guo R. Promotion effect of carbon nanotubes-doped SDS on methane hydrate formation. Energy & Fuels, 2017, 31(2): 1850–1857
32. Wang F, Song Y, Liu G Q, Guo G, Luo S J, Guo R B. Rapid methane hydrate formation promoted by Ag & SDS-coated nanospheres for energy storage. Applied Energy, 2018, 213: 227–234
33. Wang F, Jia Z, Luo S J, Fu S F, Wang L, Shi X S, Wang C S, Guo R B. Effects of different anionic surfactants on methane hydrate formation. Chemical Engineering Science, 2015, 137: 896–903
34. Prajapati R R, Bhagwat S S. Effect of foam boosters on the

micellization and adsorption of sodium dodecyl sulfate. Journal of Chemical & Engineering Data, 2012, 57(12): 3644–3650

35. Hu Z, Verheijen W, Hofkens J, Jonas A M, Gohy J F. Formation of vesicles in block copolymer-fluorinated surfactant complexes. Langmuir, 2007, 23(1): 116–122
36. Jackson A, Li P, Dong C C, Thomas R K, Penfold J. Structure of partially fluorinated surfactant monolayers at the air-water interface. Langmuir, 2009, 25(7): 3957–3965
37. Wang F, Guo G, Liu G Q, Luo S J, Guo R B. Effects of surfactant micelles and surfactant-coated nanospheres on methane hydrate growth pattern. Chemical Engineering Science, 2016, 144(144): 108–115
38. Shiloach A, Blankschtein D. Prediction of critical micelle concentrations of nonideal ternary surfactant mixtures. Langmuir, 1998, 14(15): 4105–4114
39. Evans J B, Evans D F. A comparison of surfactant counterion effects in water and formamide. Journal of Physical Chemistry, 1987, 91 (14): 3828–3829
40. Tabuteau H, Ramos L, Nakaya-Yaegashi K, Imai M, Ligoure C. Nonlinear rheology of surfactant wormlike micelles bridged by telechelic polymers. Langmuir, 2009, 25(4): 2467–2472
41. Petkova R, Tcholakova S, Denkov N D. Foaming and foam stability for mixed polymer-surfactant solutions: effects of surfactant type and polymer charge. Langmuir, 2012, 28(11): 4996–5009